Emergence and Propagation of Asynchronous States of Spontaneous Cortical Activity

Román Arango[1], Pedro Mateos-Aparicio[2], Maria V. Sanchez-Vives[2,3†] and Emili Balaguer-Ballester[1†]

(1) Department of Computing and Informatics, Faculty of Science and Technology, Bournemouth University, UK.
(2) Institut d'Investigacions Biomèdiques August Pi i Sunyer (IDIBAPS), Barcelona, Spain. (3) ICREA, Barcelona, Spain.
† Joint last author.

30th Annual Computational Neuroscience Meeting, Online, 5th July 2021

Slow Oscillations (SO) as The Default Activity Pattern of the Cerebral Cortex [1]

Phenomenology

- Multiscale Slow Oscillations (≤1Hz):
  - from the neuronal level, to the whole brain (slow waves), through the **local network level**.
- Emergent activity under functional disconnection:
  - NREM sleep, deep anaesthesia or **cortical slices**

Key Dynamical Features

- Relaxation-oscillator behaviour:
  - Intrinsic fluctuations between two alternating metastable attractors [5]: **UP and DOWN states**.
- Spatio-temporal propagation:
  - The travelling **UP/DOWN wavefront** reveals properties of the underlying network [4].

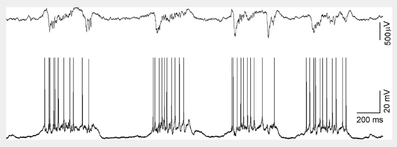

Figure 1:Simultaneous LFP (**top**) and intracellular (**bottom**) recordings from the auditory cortex of the anaesthetized rat, exhibiting slow oscillations [2]

.

Further Properties of the SO Cortical State

- Low Connectivity: resilience to perturbances [3].
- Facilitation of the transition towards more connected, awake-like states (AS).
- UP States: Model of circuit attractor implementing computation and acting as a window into conciousness.

→ **SO is a promising paradigm to study the cortical function and the emergence of conciousness.**

Motivation

How such a globally synchronized regime (the SO) gives rise to largely decorrelated awake states is an open question [5, 6, 7]. We aim at:

- *Characterising and detecting the various states emerging from the SO regime*
- *In particular, how the emergence of asynchrony is spatially orchestrated by the local network.*

Experimental Model and Cortical Slice Recordings

Extracellular recordings in coronal cortical slices of the ferret's primary visual cortex

From SO to an Awake-Like State (AS) [3, 8]

Pharmacological Modulations

- addition of Carbachol (0.5 μM) + Norepinephrine (50 μM)
- reduction of extracellular Calcium (from 1 mM to 0.8 mM)

→ Experimental model to explore the transitions from the SO state towards an awake-like, largely asynchronous state: emulating the transition from unconciousness to consiousness.

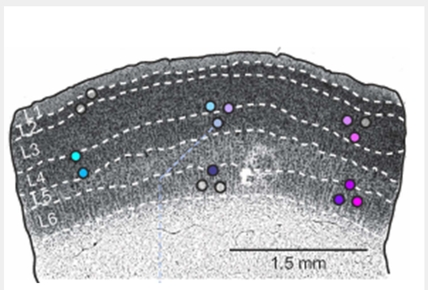

Figure 2:Nissl-stained ferret's V1 cortical slice depicting cortical layers and the location of the multi-electrode array. Electrodes will ideally lie on different layers (supra- and infragranular), across different cortical columns [4].

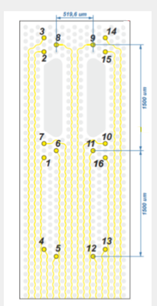

Figure 3:16-channel flexible multi-electrode array used for the recordings [9].

LFP and MUA

Extracellular Recordings are usually decomposed into Local Field Potentials (LFP) and Multi-Unit Activity (MUA):

- LFP results from afferent neuronal activity (e.g., from the summation of EPSP), as captured by the low-frequency band (<200Hz) of the extracellular recordings.
- Only units in the vicinity of the electrode contribute to the MUA (ie, efferent activity), represented in the high frequencies of the recording.

Estimating the MUA

Theoretical motivation: high-frequency spectral components of the population firing rate are asymptotically proportional to the individual firing rates of the neurons involved [10].

→ The MUA may be estimated as the relative power change of the high frequencies (200-1500 Hz) of the extracellular recordings.

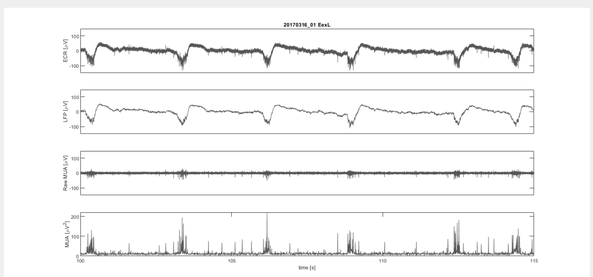

Figure 4:Signals obtained from an electrode's ECR during the SO regime. **From top to bottom**: ECR, LFP, raw MUA and energy-preserving MUA.

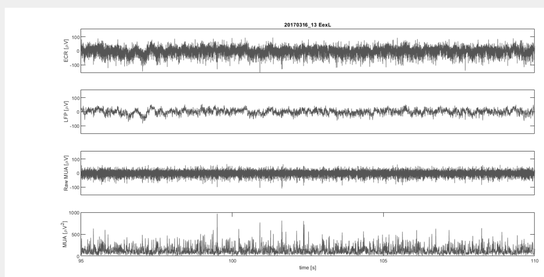

Figure 5:Same as previous figure during the Awake-Like (AS) regime. Note the change of magnitude order over the MUA signals.

Decomposition of the Awake-Like Regime into Synchronous/Asynchronous Periods

- Periods of MUA are deemed asynchronous whenever their spectral features do not significantly differ from their intrinsic background noise.
- To further validate this method, we devised a complementary strategy to detect synchronous activity, which provides in addition significance level thresholds.

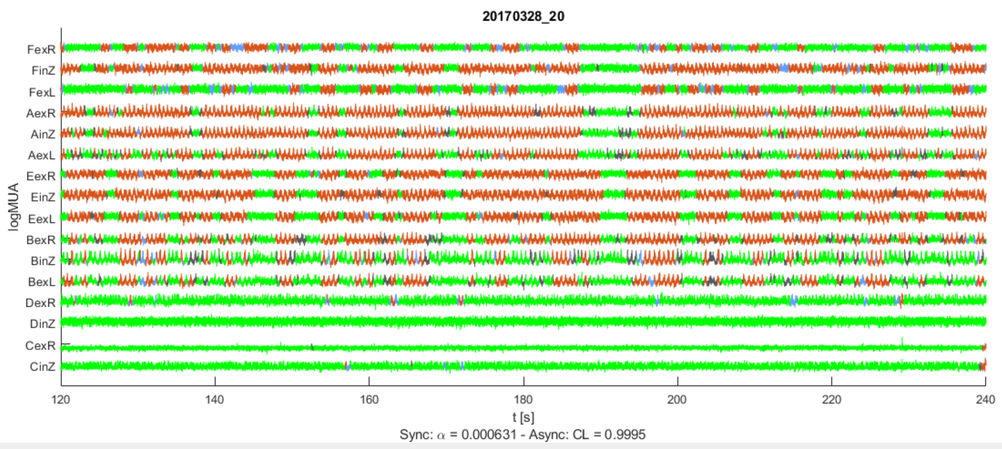

Figure 6:Representative detection example of asynchronous and synchronous states over multi-channel logMUA signals. Synchronous periods detected at the stated significance level $\alpha = 6.31 \cdot 10^{-4}$ are shown in red; asynchronous periods within a confidence level $CL = 99.95\%$, in green; in blue those periods that are over-classified; and in black, the not-classified.

Spatial Correlation of Oscillatory Activity During the AS

MUA's Power Spectra

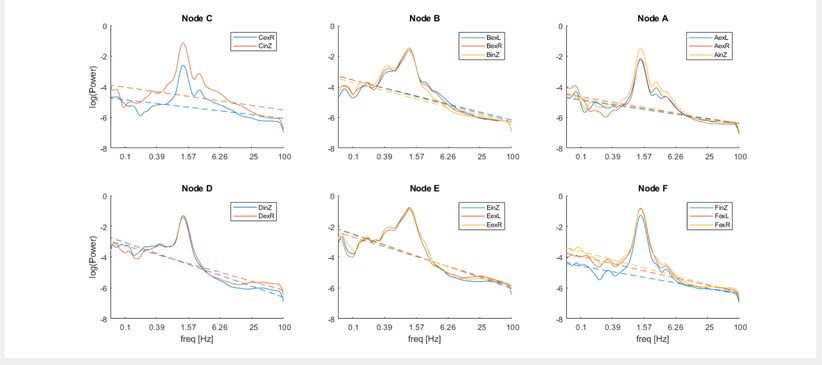

Figure 7:Averaged power spectra of the logMUA of individual channels. Log-log-space plots are displayed by MEA nodes. Dashed lines hint at their background energy.

A consistent main peak (1.482 Hz ± 0.135 Hz, $n = 5$) in all channels across different slices in estimated logMUA's power spectra over entire AS recordings (300 s) reflects the time-average of intermittent surges of oscillations.

→ Significant differences both in peak's frequency and power between intra- v inter-column location, irrespective of the layer.

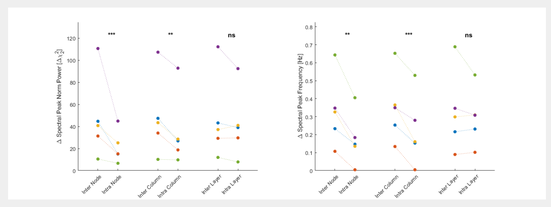

Figure 8:Effects of the layout spatial organisation over the main spectral peak's frequency (**right**) and normalised power (**left**). Each dot represents the marginal mean of the corresponding feature for each slice under one level of the 2-level location factor. (*) $p < 0.05$, (**) $p < 0.01$, (***) $p < 0.001$.

Spatial Clustering of Spectral Densities

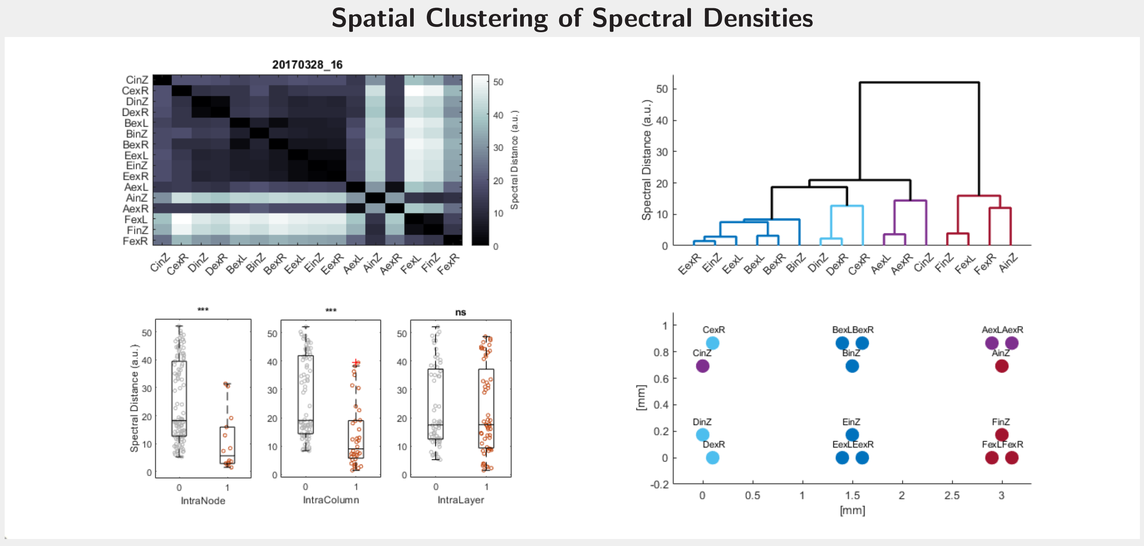

Figure 9:Spatial organisation of mean oscillatory activity assessed by the similarity of normalised power spectra. **Top left**, similarity heat-map of all 16 channels' spectra; the darker the matrix entry, the more similar the spectra. **Bottom left**, statistical assessment of the median similarity distance under three distinct organisational levels (node, column and layer). Each dot represents the similarity between two power spectra. Grey dots for inter-group comparisons, red for intra-group. (***) $p < 0.001$. **Top right**, dendrogram representation of the similarity matrix. Four non-degenerated clusters were obtained, whose colour-coding matches that of the MEA schematic below (**bottom right**).

→ Power spectra tend to form clusters that broadly encompass cortical columns, as intra-column v inter-column similarity tests show.
→ The laminar level proves not to be significant to account for spectral similarity.

Global Spatio-Temporal Coherence of Asynchronicity

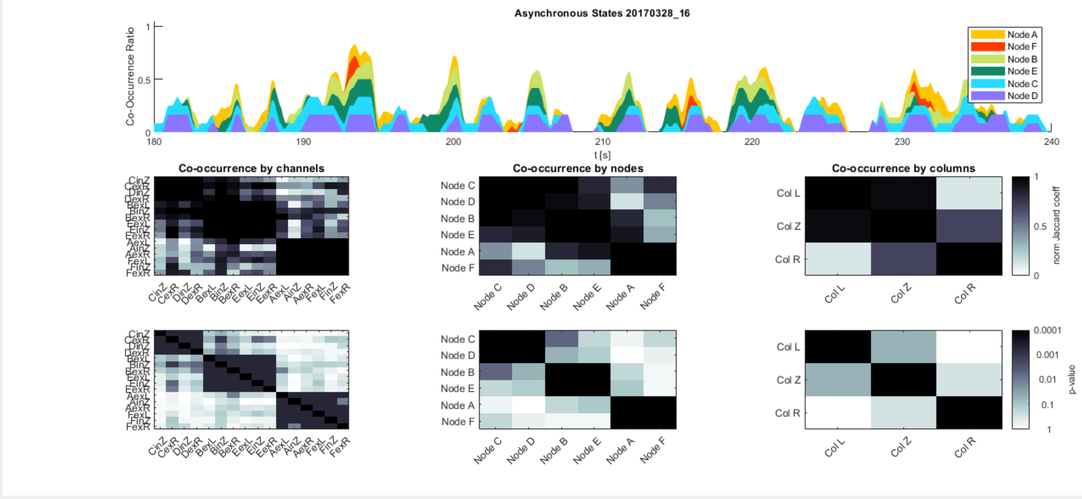

Figure 10:Spatio-temporal coherence of asynchronous states' occurrence. **Top**: isolated async states, aggregated by node (as their colour indicates) and overlapped for all 6 nodes. **Bottom**: similarity matrices for each level of aggregation: channel (**left**), node (**centre**) and column (**right**). **Top row** shows the normalised Jaccard coefficients, measuring the ratio between the intersection and union of two sets. Normalisation of the Jaccard coefficients is required to compare asynchronous patterns of aggregates with very disparate synchronicity tenors. **Bottom row** shows the corresponding surrogate p-values (N = 10000, for column and node aggregates; N=1000 for the individual channel interactions).

- Channels within the same node or the same column show the highest degree of co-occurrence of asynchronous periods.
- Some evidences of transient trans-columnar asynchrony co-occurrence.

→This is the first step towards our proof that transitions between synchronous and asynchronous states propagate underlying a columnar organisation.

Conclusions

- In the AS, an excited SO-like activity cohabits with periods of asynchrony of uneven duration and irregular occurrence [5].
- The spatio-temporal interplay of these states depends on the structural organisation of the cortical network:
  - the firing rate intensity is dictated by the layer [11]
  - the oscillatory activity is sustained at the column level [12]
  - sync/async alternation propagates across the whole slice

References

[1] Sanchez-Vives MV, et al. (2017) Neuron 94(5):993-1001.
[2] Sanchez-Vives MV, et al. (2014) Arch Ital Biol. 152(2-3):147-55.
[3] D'Andola M, et al. (2017) Cereb Cortex, 112:105-113.
[4] Capone C, et al. (2017) Cereb Cortex, 28:1-17.
[5] Tort-Colet N, et al. (2021) Cell Reports 35:109270
[6] Dasilva M, et al. (2021) Neuroimage 224:117415.
[7] Barbero-Castillo A, et al. (2021) Adv Sci (Weinh) 2021 May 21:e2005027.
[8] Barbero-Castillo A, et al. (2021) J Neurosci, 41(23):5029-5044.
[9] Illa X, et al. (2015) In: SPIE Microtechnologies, Int Soc Opt and Phot, p. 951803.
[10] Mattia M, et al. (2002) Phys Rev E, 66 051917.
[11] Senzai Y, et al. (2019) Neuron 101(3):500–513.
[12] Rebollo B, et al. (2021) Sci Adv 7(10):eabc7772.